15. THERMOBAROMETRIC CALCULATION OF PEAK METAMORPHIC CONDITIONS OF THE SULLIVAN DEPOSIT

Glen R. De Paoli[1] and David R.M. Pattison[2]

1 2739 4th Ave N.W., Calgary, Alberta T2N 0P9
2 Department of Geology and Geophysics, The University of Calgary, 2500 University Drive N.W., Calgary, Alberta T2N 1N4

ABSTRACT

The Sullivan Zn-Pb-Ag mine in southeastern British Columbia is a mid-Proterozoic sedimentary exhalative deposit that has been metamorphosed to transitional greenschist-amphibolite grade. The mineral textures are predominantly of metamorphic origin. There are no significant differences in silicate mineral compositions between sulphide-rich lithologies and silicate-rich lithologies. High modal abundance of Mn-rich garnet in some rocks indicates a Mn-rich phase was likely part of the pre-metamorphic mineral assemblage. Metamorphic conditions were estimated using multi-equilibrium thermobarometric techniques involving silicate-carbonate equilibria. Peak metamorphic temperature estimated by the garnet-biotite Fe-Mg exchange equilibrium is 450°C ± 50°C. Lower temperature estimates from some samples are interpreted to record the temperature of cessation of garnet growth prior to the attainment of peak metamorphic temperature. Peak metamorphic pressure determined from equilibria applicable to the assemblage garnet-biotite-muscovite-chlorite-calcite-quartz-fluid is 380 MPa ± 100 MPa (equivalent to approximately 14 km of burial). The fluid composition accompanying this pressure estimate is $XH_2O = 0.38$, $XCO_2 = 0.62 \pm 0.07$. The P-T estimates are consistent with burial metamorphism during Proterozoic times.

INTRODUCTION

The Sullivan mine, in southeastern British Columbia, is a sedimentary exhalative Zn-Pb-Ag orebody which was deposited in mid-Proterozoic times. Regional metamorphic grade in the vicinity of the orebody is greenschist facies (biotite-chlorite), but amphibolite grade areas containing garnet and sillimanite occur in the Mathew Creek area approximately 10 km to the southwest (Leech, 1962; McFarlane and Pattison, 2000; Fig. 15-1). The deposit itself is anomalous with respect to the immediately surrounding rocks in that it contains abundant metamorphic garnet.

Many characteristics of the deposit have been affected by the metamorphism, including fluid inclusions, stable isotopes, and the textures and mineralogy of the ore, gangue, and pre-metamorphic hydrothermal alteration zones. An important step in understanding the effects of a metamorphic overprint is a well-constrained estimate of metamorphic temperature, pressure, and fluid composition (P-T-X).

Previous estimates of metamorphic conditions for the Sullivan deposit are summarized in Table 15-1. Until this study, no attempt has been made to estimate metamorphic conditions using the techniques of multi-equilibrium thermobarometry applied to the silicate-carbonate minerals in the orebody. An estimate by these methods has the advantage of determining temperature, pressure, and fluid composition simultaneously. Some of the information in this contribution is presented in detail in De Paoli and Pattison (1995). Mineral abbreviations are given in Table 15-2. Sample locations are given in Figure 15-2.

PETROGRAPHY

Samples were classified into three rock types on the basis of bulk mineralogy: silicate matrix rocks, sulphide matrix rocks, and amphibolite. None of the samples used for P-T-X estimates shows any textural or compositional evidence of retrograde alteration. Localized retrograde alteration is found in the southeast section of the orebody (Ethier et al., 1976; Campbell and Ethier, 1983). Mineralogical evidence includes: chloritized biotite; biotite with compositional zoning; stilpnomelane overgrowths on sulphides and silicates; hematite staining; and poikilitic magnetite grains enclosing pyrite.

Silicate matrix rocks

Silicate matrix rocks are represented by the 'waste beds' (sulphide poor siliciclastic interbeds) within the bedded ore and contain less than 10% sulphides. The overall mineral assemblage is Qtz + Ms ± Bt ± Chl ± Grt ± Pl ± Cal, with Po ± Py ± Sph ± Gn.

Porphyroblasts

Porphyroblasts in silicate matrix rocks include garnet, biotite, chlorite, and calcite. In some samples, distinguishing between porphyroblasts and matrix was not feasible due to uniformity of grain size. Garnet is found in most samples and its abundance and grain size is approximately proportional to sulphide abundance. Garnets range from 0.1 to 1.0 mm in diameter and occur as isolated idiomorphic grains with inclusion-rich cores, and as aggregates of poikiloblastic grains rimming pyrrhotite laths (Fig. 15-3a). Garnet inclusions include quartz, calcite, chlorite, and pyrrhotite. Biotite and chlorite porphyroblasts occur as randomly oriented idiomorphic grains up to 1.0 mm across. Calcite is rare

De Paoli, G.R. and Pattison, D.R.M.
2000: Thermobarometric Calculation of Peak Metamorphic Conditions of the Sullivan Deposit; in The Geological Environment of the Sullivan Deposit, British Columbia, (ed. J.W. Lydon, J.F. Slack, T. Höy and M.E. Knapp; Geological Association of Canada, Mineral Deposits Division, MDD Specal Volume No. 1, p.

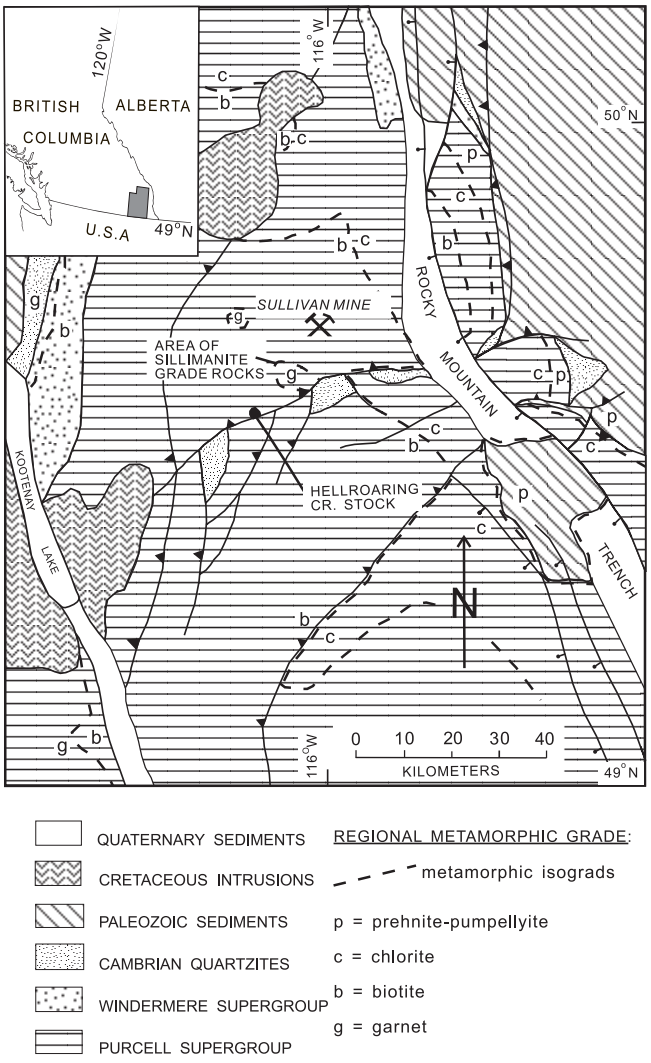

Figure 15-1. Simplified geological map of the Sullivan Mine Region (Leech, 1957, 1962; Reesor, 1973; Höy, 1993; Höy et al, 1995; Read et al. 1991).

among the silicate matrix samples examined (2 out of 9 samples, with 9 and 3 mode % calcite respectively). In places where it was found, it ranges from matrix size to 0.5 mm, with the larger grains commonly rimming pyrrhotite laths.

Matrix

The matrix is composed of roughly equal amounts of fine-grained (10 to 50 μm) quartz and muscovite. In some rocks, biotite and chlorite are fine-grained enough to be considered matrix rather than porphyroblasts. Many quartz grains show undulose extinction and annealed textures. Plagioclase, possibly peristerite, *(see* Mineral Chemistry section *below*) was identified in the matrix of one sample with the electron microprobe. Accessory minerals include sulphides (mostly pyrrhotite laths oriented parallel to bedding), titanite, apatite, and zircon.

Sulphide Matrix Rocks

Sulphide matrix rocks include samples from the sulphide-rich layers in the bedded ore and contain > 40% sulphide minerals. The overall mineral assemblage is Po ± Sph ± Gn

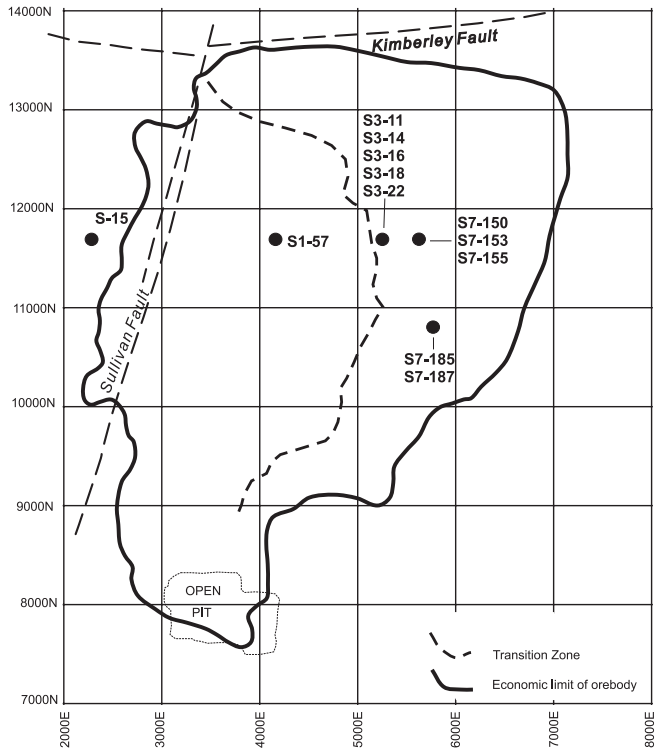

Figure 15-2. Outline of the Sullivan orebody showing sample locations. Samples DS-47, DS-85, and UCG-84 are from bedded ore on the eastern margin of the deposit, but their exact locations are uncertain.

± Py ± Grt ± Bt ± Ms ± Qtz ± Chl ± Cal. Differentiation of matrix vs. porphyroblasts was not always possible due to complex sulphide mineral textures and the broad range in size of both the sulphide and silicate minerals.

Sulphide Minerals

The major sulphide minerals include pyrrhotite, sphalerite, galena (± boulangerite), and minor pyrite. The sulphide minerals show the following varieties: anhedral equigranular pyrrhotite, galena, and sphalerite; massive pyrrhotite or sphalerite containing small anhedral blebs of sphalerite, pyrrhotite, or galena; and a crudely banded texture of anhedral pyrrhotite, sphalerite, and galena. Pyrite usually exhibits a euhedral, porphyroblastic texture.

Silicate and Carbonate Minerals

Silicate and carbonate minerals in sulphide matrix rocks include quartz, muscovite, garnet, biotite, and chlorite, and carbonate minerals with varying amounts of Ca, Fe, Mg, and Mn (*see* Mineral Chemistry section *below*). Silicate and carbonate minerals tend to be coarser-grained and less euhedral than in silicate matrix rocks. Carbonate minerals are more abundant than in silicate matrix rocks (2 of three samples with 10 mode % carbonate in each compared to values given above for silicate matrix rocks). Quartz and carbonate are generally anhedral. Larger and more euhedral garnet, biotite, muscovite, and chlorite porphyroblasts reach 2 mm in size. Garnet-rich laminae are commonly found at the contact between sulphide-rich and silicate-rich bands (Fig. 15-3b).

Table 15-1. Previous estimates of metamorphic conditions for the Sullivan Orebody.

method	temperature (°C)	pressure (MPa)	reference
oxygen isotope fractionation between quartz and magnetite	400 - 560		Ethier et al. (1976)
sulphur isotope fractionation between sphalerite and galena	300 - 340		Ethier et al. (1976)
arsenopyrite geothermometer (Kretschmar and Scott, 1976)	400 - 490		Ethier et al. (1976)
sphalerite geobarometer (Scott, 1973)		500	Ethier et al. (1976)
fluid inclusions in quartz	200 - 415		Leitch (1992)
sphalerite geobarometer (Toulmin et al. 1991)	375	450	Lydon and Reardon (2000)

Amphibolite

The amphibolite represents metamorphosed gabbro and diorite rocks of the Moyie sills which intrude the western edge of the deposit. Metamorphic minerals and textures in this sample have overprinted most of its original igneous character. The rock is composed of equigranular, subhedral to euhedral amphibole, chlorite, quartz, plagioclase, clinozoisite, and calcite. Plagioclase shows complex textures (*see* Mineral Chemistry section *below*) and is strongly sericitized. Pyrrhotite and ilmenite are disseminated throughout. Ilmenite is nearly always rimmed by titanite and/or clinozoisite.

MINERAL CHEMISTRY

Minerals were analyzed by electron microprobe at the University of Calgary. Analytical methods are described in De Paoli and Pattison (1995). Full mineralogical compositions are given in Appendix 12.

In many metamorphosed sulphide ore deposits, particularly those of higher metamorphic grade, silicate minerals such as garnet, biotite and chlorite tend to be more Mg-rich and less Fe-rich in sulphide-rich rocks than in sulphide-poor rocks (Froese, 1969; Bachinski, 1976; Hutcheon, 1979; Nesbitt, 1982). Within the Sullivan deposit there are differences in mineral composition between silicate-rich and sulphide-rich rocks, but two distinct populations of Fe/(Fe+Mg) ratios cannot be discerned.

As an example, figure 15-4 shows Fe/(Fe+Mg) vs. Xsps in garnet rims for both the silicate and sulphide lithologies (analyses in Table 15-3). Although the range of Fe/(Fe+Mg) ratios for garnets in sulphide-rich rocks is slightly lower (from 0.888 to 0.953) than in silicate rocks (from 0.904 to 0.963), there is a large overlap in the range of values between the two rock types. There is similar overlap in the variation of manganese content in garnet, with Xsps in sulphide-rich rock ranging from 0.277 to 0.518, and Xsps in silicate-rich rocks ranging from 0.090 to 0.454. Biotite compositions show a similar trend in Fe/(Fe+Mg) as garnet. The range of Fe/(Fe+Mg) in biotite in sulphide-rich rocks (from 0.315 to 0.596) is lower than in silicate-rich rocks (from 0.396 to 0.687), but the range of overlap is large.

Electron microprobe examination identified fine-grained (50 μm) plagioclase in the matrix of one silicate matrix sample. Compositions within a single grain and between grains range from pure albite to an_{28} (total of 78 analyses), with a compositional gap between an_3 and an_{13} (one value of an_7). The virtual absence of analyses between an_3 and an_{13} suggests the presence of peristerite. Peristerite is plagioclase in which albitic and more intermediate (more Ca-rich) plagioclase coexist, with exact compositions controlled by a pressure-temperature sensitive solvus. However, at 450ºC and 380 MPa (the preferred P-T estimate, *see* P-T-X Estimate section *below*) the peristerite gap spans approximately an_3 to an_{20}, not an_3 to an_{13} (Crawford, 1966; Maruyama et al. 1982). The possibility exists that the plagioclase compositions may represent not only metamorphic peristerite, but also relict igneous compositions and albite, the latter related to pre-metamorphic hydrothermal alteration. Interpretation of the significance of the compositional gap with respect to metamorphic temperature and pressure requires reliable interpretation of peristerite textures. Efforts to image the textures of individual feldspar grains with a scanning electron microscope were unsuccessful due to small grain size and the very slight contrast in mean atomic number between minerals so close in chemical composition. Similar attempts to determine compositional/textural relationships for plagioclase in the amphibolite were also unsuccessful, with compositions ranging from pure albite to an_{17} with no compositional gap. Consequently, we feel that we do not sufficiently understand the plagioclase relations to use them for P-T interpretations.

Carbonate analyses differ noticeably between silicate matrix and sulphide matrix rocks. The composition of carbonate in silicate matrix rocks is near pure calcite, with less than 2 wt.% combined FeO, MgO, and MnO. Carbonate in sulphide matrix rocks have significant siderite (up to 14.21 wt.% FeO), dolomite (up to 15.98 wt.% MgO), and rhodocrosite (up to 4.58 wt.% MnO) components.

P-T-X Estimate

Metamorphic pressure, temperature and fluid composition estimates were made using the multi-equilibrium thermo-

Table 15-2. Mineral, end members, and abbreviations (after Kretz, 1983).

mineral	symbol	end member	symbol
garnet	Grt	almandine (Fe)	alm
		pyrope (Mg)	prp
		spessartine (Mn)	sps
		grossular (Ca)	grs
biotite	Bt	annite (Fe)	ann
		phlogopite (Mg)	phl
plagioclase	Pl	anorthite (Ca)	an
		albite (Na)	alb
		orthoclase (K)	or
chlorite	Chl	clinochore (Mg)	cln
		daphnite (Fe)	dph
muscovite	Ms		
calcite	Cal		
quartz	Qtz		
pyrrhotite	Po		
pyrite	Py		
sphalerite	Sph		
galena	Gn		

Table 15-3. Selected garnet-biotite compositional data and temperatures at 380 MPa from the Berman (1990) calibration of the garnet-biotite Fe-Mg exchange geothermometer. Data for rim analyses unless otherwise indicated.

		Garnet[b]					Biotite[c]						
sample	lithology[a]	XFe	XMg	XMn	XCa	Fe/ Fe+Mg	XFe	XMg	XAl^{VI}	XTi	Fe/ Fe+Mg	mode % Chl[d]	T (°C)
S1-57	silicate	0.359	0.038	0.454	0.138	0.904	0.334	0.514	0.103	0.033	0.394	trace	377
S3-11	silicate	0.726	0.031	0.143	0.100	0.959	0.598	0.267	0.095	0.032	0.691	5	460
(core)		0.678	0.028	0.198	0.096	0.960							448
S3-14	sulphide	0.338	0.038	0.518	0.106	0.899	0.284	0.617	0.061	0.022	0.315	----	296
S3-16	silicate	0.723	0.028	0.219	0.024	0.963	0.590	0.256	0.112	0.025	0.697	----	411
S3-18	sulphide	0.666	0.033	0.277	0.017	0.953	0.518	0.351	0.080	0.041	0.596	15	364
(core)		0.631	0.024	0.285	0.051	0.963							330
S3-22	silicate	0.609	0.031	0.320	0.037	0.952	0.497	0.356	0.107	0.027	0.583	----	365
S7-150	silicate	0.566	0.043	0.337	0.040	0.929	0.504	0.350	0.092	0.039	0.590	20	451
S7-153	silicate	0.610	0.055	0.294	0.034	0.917	0.464	0.393	0.098	0.031	0.541	5	448
S7-155	silicate	0.604	0.050	0.277	0.057	0.924	0.441	0.413	0.102	0.028	0.516	trace	416
(core)		0.568	0.049	0.273	0.098	0.921							439
DS-47	silicate	0.752	0.036	0.123	0.084	0.954	0.551	0.303	0.105	0.036	0.645	40	431
DS-85	silicate	0.783	0.036	0.090	0.084	0.956	0.572	0.273	0.117	0.032	0.677	40	456
(core)		0.509	0.018	0.228	0.172	0.966							403
UCG-84	sulphide	0.427	0.054	0.476	0.036	0.888	0.341	0.531	0.092	0.021	0.391	----	385
(core)		0.304	0.031	0.563	0.093	0.907							358

[a]indicates silicate matrix or sulphide matrix rock
[b]$Xi = i/(Fe^{2+} + Mg + Mn + Ca)$
[c]$Xi = i/(Fe + Mg + Mn + Al^{VI} + Ti)$
[d]by visual estimation

barometric computer program TWEEQU, version 1.02 (Berman, 1988, 1991). A description of the method is provided in Berman (1991). Most samples only contained sufficient mineral phases to obtain a temperature estimate (garnet-biotite Fe-Mg exchange). One sample, containing the mineral assemblage Grt-Bt-Ms-Chl-Cal-Qtz, allowed a complete P-T-X estimate.

Geothermometry

Table 15-3 shows selected garnet and biotite compositions and temperature estimates (assuming a pressure of 380 MPa) for 12 samples. Temperature estimates range from 296 to 460ºC. De Paoli and Pattison (1995) argued that the most likely explanation for the range in temperature estimates was that garnet stopped growing prior to the attainment of peak metamorphic temperature in those samples giving lower temperature estimates.

Some garnets may have stopped growing earlier than others due to the loss of a reactant phase involved in garnet growth - in particular, the phase or phases supplying manganese. Garnet has been shown to be stable at lower temperatures in a geochemical system containing manganese than in a pure Fe-Mg system (Symmes and Ferry, 1992). Figure 15-1 shows garnet is not part of the regional metamorphic assemblage in the immediate vicinity of the Sullivan orebody. Consequently, the most likely explanation for the presence of garnet within the orebody is anomalously Mn-rich bulk rock compositions within the deposit compared to the Aldridge Formation in general.

Several reactant phases may have supplied manganese to the garnets in the deposit. The high manganese content and high modal abundance of garnet in many samples, especially sulphide-matrix samples (e.g. 37 wt. % MnO and 85 mode % garnet in one sample), requires a Mn-rich reactant phase, such as rhodochrosite ($MnCO_3$), or pyrolusite (MnO_2). Pyrolusite, or other oxides, are unlikely to have been present in the deposit prior to metamorphism because of the reducing conditions of the sediments (W. Goodfellow, pers. comm., 1995). Reactions involving rhodochrosite and detrital clay minerals (represented by kaolinite below) may have produced Mn-rich garnet by a reaction of the type:

(1) $$3MnCO_3 + Al_2Si_2O_5(OH)_4 + SiO_2 = Mn_3Al_2Si_3O_{12} + 3CO_2 + 2H_2O$$

$$(\text{rhodochrosite}) + (\text{kaolinite}) + (\text{quartz}) = (\text{spessartine}) + (CO_2) + (H_2O)$$

Relatively manganese-rich carbonate (4.58 wt.%) was identified in a sulphide matrix rock (*see* Mineral Chemistry section *above*), further suggesting that Mn-carbonates may have been a significant part of the original depositional mineralogy of the deposit.

Petrographic evidence indicates chlorite may also have been an important reactant phase during garnet growth. Those samples which give low temperature estimates (< 430ºC) contain little or no chlorite, whereas samples giving higher temperature estimates (> 430ºC, including all five samples selected for the temperature estimate, *see below*) contain significant chlorite (5 - 40 mode %). Garnet growth may have occurred via a chlorite-consuming reaction of the type:

(2) $$\text{Chlorite(Mn)} + \text{muscovite} + \text{quartz} = \text{garnet (Mn)} + \text{biotite} + H_2O$$

and ceased at the temperature at which the chlorite was exhausted. In those rocks containing a low modal abundance of relatively Mn-poor garnet, reaction (2) alone may have produced the garnets, whereas in rocks with higher modal abundance of relatively Mn-rich garnet, reaction (2) may have proceeded either simultaneously with, or follow-

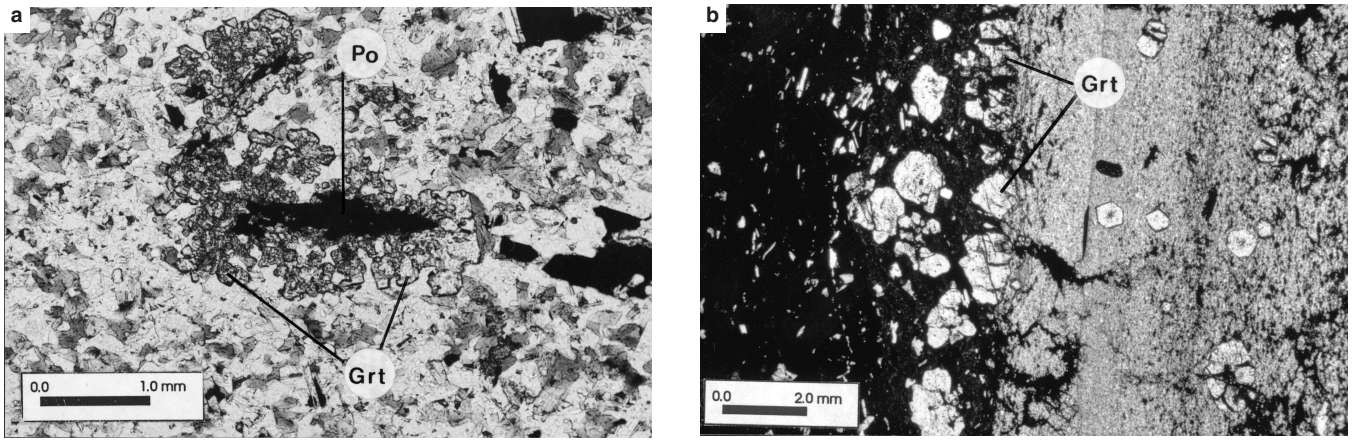

Figure 15-3. Photomicrographs of typical mineral textures in the Sullivan orebody. **(a)** Sample S3-11 from a waste band within the bedded ore showing garnet (Grt) rimming pyrrhotite (Po). **(b)** Sample UCG-84, garnets (Grt) concentrated along contact between silicate waste layer and sulphide layer within bedded ore.

ing, the completion of reaction (1). Sphalerite and pyrrhotite may also have been subordinate sources of manganese.

A temperature estimate for the deposit of 450ºC ± 50ºC was made from the average of the five highest estimates, samples S3-11, S7-150, S7-153, DS-47, and DS-85. The quoted uncertainty results from recalculating the equilibria at two standard deviations of the mineral analyses (Ferry and Spear, 1978).

Geobarometry

Among the many different rock types examined from the Sullivan deposit, only one sample with a mineral assemblage suitable for geobarometry was identified. This is sample S3-11 from a silicate matrix rock with the mineral assemblage Grt-Bt-Ms-Chl-Cal-Qtz. Equivocal feldspar textures and compositions (*see* Mineral Chemistry section *above*) did not allow application of pressure-sensitive, fluid composition-independent equilibria involving plagioclase end members. In sample S3-11, three locations were selected where all the minerals of interest were in close proximity. Each location was treated as a separate chemical system, and the P-T-XCO_2 determination for each location was averaged to determine the P-T-XCO_2 estimate for the sample. This approach accounts for small scale variations in bulk composition within the sample. Pressure-temperature, pressure-XCO_2, and temperature-XCO_2 diagrams for location #2 in sample S3-11 are given in Figures 15-6a,b and c respectively. A summary of the P-T-X results for all three locations in sample S3-11 are given in Table 15-4.

With the exception of the garnet-biotite Fe-Mg equilibrium (curve #1 in Figures 15-6a,b,c), equilibria from the mineral assemblage Grt-Bt-Ms-Chl-Cal-Qtz involve a fluid phase. The position of the curves for these equilibria on P-T-X diagrams changes as the H_2O/CO_2 ratio of the fluid is varied. Without an independent determination of the metamorphic fluid composition, the H_2O/CO_2 ratio which gave the tightest intersection of the equilibrium curves was selected. The high angle of intersection of the equilibrium curves in Figure 15-6b demonstrates that the equilibrium fluid composition is tightly constrained, as even a small variation of the H_2O/CO_2 ratio destroys the tight intersection.

The average pressure estimate of the three locations in sample S3-11 is 380 MPa ± 100 MPa (Table 15-4). The uncertainty results from recalculating the equilibrium at two standard deviations of the mineral analyses.

Fluid Composition

The average of the fluid compositions from the three locations in sample S3-11 is $XH_2O = 0.38$, $XCO_2 = 0.62$ (Table 15-4). The deviation of the maximum XH_2O (0.44) and the minimum XH_2O (0.31) from the mean XH_2O (0.38) between the three determinations, a value of ± 0.07, is taken as an indication of the uncertainty in the fluid composition estimate. This relatively CO_2-rich fluid estimate is particular to this sample, and is not necessarily representative of metamorphic fluid compositions for the whole deposit.

The pressure estimate was calculated assuming the metamorphic fluid was an H_2O-CO_2 binary. This assumption is reasonable, as the concentration of other possible fluid phases such as CO, CH_4, H_2, H_2S, SO_2 and COS determined using the computer software and fluid property data of Connolly and Cesare (1993) is negligible (Table 15-5). The values in Table 15-5 were generated assuming the presence of graphite and a pyrite-pyrrhotite sulphur activity buffer so as to give the maximum possible concentrations of the trace fluid phases. C-O-H-S trace species concentrations in the metamorphic fluid do not reach significant concentrations at this metamorphic grade regardless of the H_2O/CO_2 ratio, and therefore metamorphic fluids for the deposit as a whole were likely an H_2O/CO_2 binary.

While an XCO_2 of 0.62 may seem high for greenschist grade rocks, carbonate is a significant component of the bulk mineralogy of the Sullivan orebody (Hamilton et al. 1982,

Table 15-4. Temperature, pressure and fluid composition estimates. Sample S3-11.

location	temperature (ºC)	pressure (MPa)	XH_2O
1	470	480	0.44
2	460	360	0.38
3	450	300	0.31
average	460	380	0.38

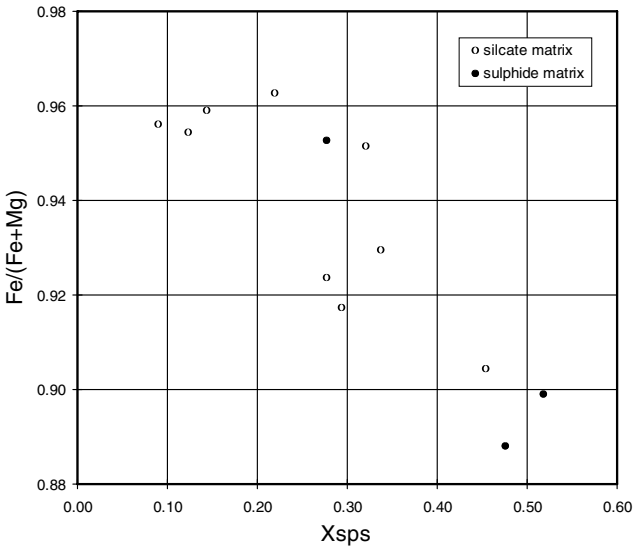

Figure 15-4. Fe/(Fe+Mg) vs. Xsps in garnet. Rim analyses plotted. Open circles denote silicate matrix samples, filled circles denote sulphide matrix samples. While garnets in a sulphide matrix tend to have lower Fe/(Fe+Mg) and higher Xsps than garnets in a silicate matrix, the broad range of compositions from both rock types overlap significantly. Garnets with higher Xsps have lower Fe/(Fe+Mg) in both rock types.

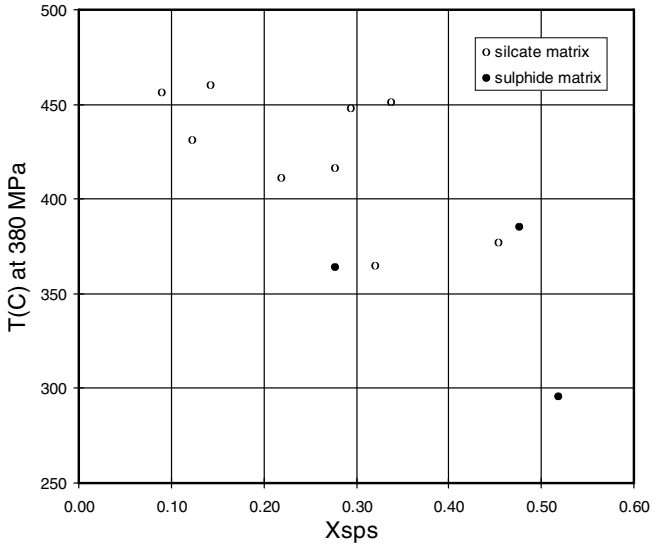

Figure 15-5. Temperature estimate (°C) at 380 MPa vs. Xsps in garnet, using rim analyses. Temperature estimate from the Berman (1990) calibration of the garnet-biotite Fe-Mg exchange geothermometer. See Table 15-1 for garnet and biotite compositional data. Figure shows lower temperature estimates come from samples with higher Xsps in garnet.

Leitch, 1992), and may have been more abundant in the pre-metamorphic mineral assemblage. Significant CO_2 will have been introduced into the metamorphic fluid via reaction (1) shown above.

DISCUSSION

There is considerable uncertainty as to the age of metamorphism of the Sullivan deposit. The Sullivan region has a long and complex tectonic and thermal history, and several metamorphic episodes have been inferred: ca. 1330 Ma (Ryan and Blenkinsop, 1971; Ross et al., 1992; Schandl et al., 1993; Anderson and Parrish, 2000; McFarlane and Pattison, 2000; Schandl and Davis, 2000); ca. 1050 - 1100 Ma (Anderson and Parrish, 2000); and Jurassic-Cretaceous time (McMechan and Price, 1982; Lydon and Reardon, 2000). The age of the peak metamorphic event at Sullivan (and possible subsequent ones) would best be determined by a pressure, temperature, and fluid composition estimate made from a mineral assemblage which includes a metamorphic mineral from which an age can be determined, such as titanite, but to date this has not been accomplished.

The metamorphic pressure estimate of 380 MPa is equivalent to approximately 14 km of lithostatic load (assuming an average rock density of 2.7 g/cm^3). For 450°C, this gives a geothermal gradient of 32°C/km, similar to the average geothermal gradient today of 30°C/km (Best, 1982), and consequently, consistent with burial metamorphism. With respect to the timing of metamorphism, 14 km of burial is in accord with the estimated thickness of Purcell Supergroup sediments overlying the deposit (Höy et al, 1995, Höy, pers. comm., 1997). However, there remains the question of unknown thicknesses of sediment removed at numerous unconformities within the Purcell Supergroup and younger strata.

Taking into consideration the maximum limit of the pressure estimate (380 MPa+ 100 MPa = 480 MPa), a pressure of 480 MPa is equivalent to 18 km of burial and gives a geothermal gradient of only 25°C/km. Eighteen km of burial is close to an estimate of 17 km of burial during Jurassic-Cretaceous times for the Mount Fisher area, 35 km east of the Sullivan deposit (McMechan and Price, 1982). While there is evidence for Mesozoic deformation and retrograde metamorphism of the Sullivan orebody, both are interpreted to post-date maximum metamorphic conditions (McClay, 1983; Lydon and Reardon, 2000).

The minimum limit of the pressure estimate (380 MPa - 100 MPa = 280 MPa) gives a geothermal gradient of 45°C/km, which would almost certainly require a thermal anomaly. Causes for a thermal anomaly could include magmatic intrusions (e.g. the nearby Hellroaring Creek stock) or heat associated with a possible Proterozoic orogenic event (McFarlane and Pattison, 2000).

Table 15-5. Fluid species concentrations for sample S3-11. XH_2O and XCO_2 from TWEEQU software (Berman, 1988, 1991), others from Connolly and Cesare (1993). Not normalized to 100%.

species	mole fraction
H_2O	0.32
CO_2	0.68
CO	$1.25 * 10^{-4}$
CH_4	$3.07 * 10^{-4}$
H_2	$5.74 * 10^{-5}$
H_2S	$1.31 * 10^{-3}$
SO_2	$6.22 * 10^{-10}$
COS	$3.30 * 10^{-5}$

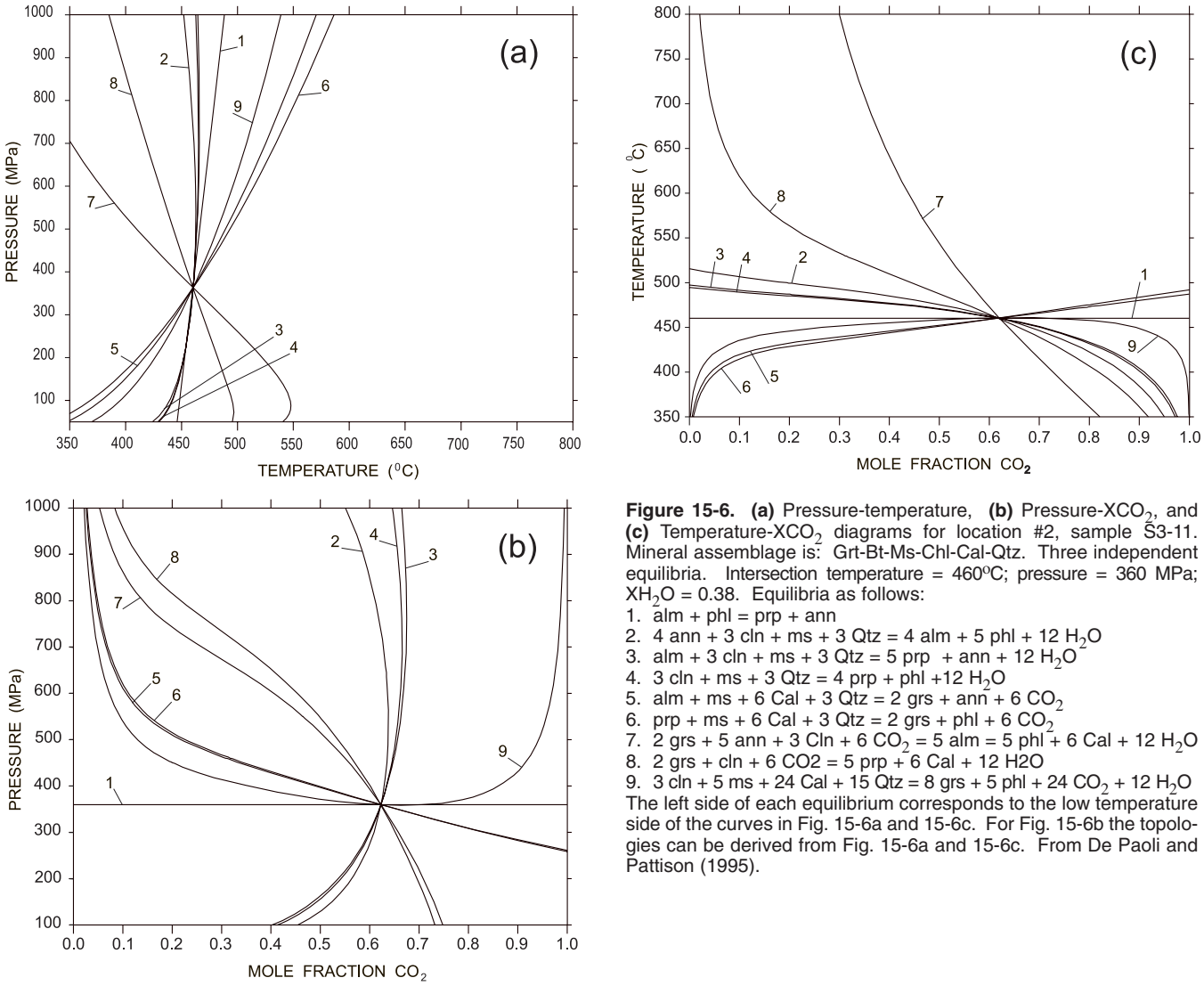

Figure 15-6. **(a)** Pressure-temperature, **(b)** Pressure-XCO_2, and **(c)** Temperature-XCO_2 diagrams for location #2, sample S3-11. Mineral assemblage is: Grt-Bt-Ms-Chl-Cal-Qtz. Three independent equilibria. Intersection temperature = 460°C; pressure = 360 MPa; XH_2O = 0.38. Equilibria as follows:

1. alm + phl = prp + ann
2. 4 ann + 3 cln + ms + 3 Qtz = 4 alm + 5 phl + 12 H_2O
3. alm + 3 cln + ms + 3 Qtz = 5 prp + ann + 12 H_2O
4. 3 cln + ms + 3 Qtz = 4 prp + phl +12 H_2O
5. alm + ms + 6 Cal + 3 Qtz = 2 grs + ann + 6 CO_2
6. prp + ms + 6 Cal + 3 Qtz = 2 grs + phl + 6 CO_2
7. 2 grs + 5 ann + 3 Cln + 6 CO_2 = 5 alm = 5 phl + 6 Cal + 12 H_2O
8. 2 grs + cln + 6 CO2 = 5 prp + 6 Cal + 12 H2O
9. 3 cln + 5 ms + 24 Cal + 15 Qtz = 8 grs + 5 phl + 24 CO_2 + 12 H_2O

The left side of each equilibrium corresponds to the low temperature side of the curves in Fig. 15-6a and 15-6c. For Fig. 15-6b the topologies can be derived from Fig. 15-6a and 15-6c. From De Paoli and Pattison (1995).

CONCLUSIONS

The Sullivan orebody has been metamorphosed to transitional greenschist-amphibolite facies (chlorite-biotite-garnet). Mineral textures in the deposit are primarily of metamorphic origin. The abundance of garnet within the deposit compared to the regional chlorite-biotite assemblage is likely due to more Mn-rich bulk compositions within the orebody. The high modal abundance of Mn-rich garnet in some rocks indicates a Mn-rich phase was likely part of the pre-metamorphic mineral assemblage. Peak metamorphic P-T-X conditions were estimated using TWEEQU computer software (Berman, 1991). Peak metamorphic temperature from garnet-biotite Fe-Mg exchange equilibrium is 450°C ± 50°C. Lower temperature estimates from some samples are interpreted to record the temperature of cessation of garnet growth prior to peak metamorphic conditions. Peak metamorphic pressure determined from the assemblage garnet-biotite-muscovite-chlorite-calcite-quartz is 380 MPa ± 100 MPa (equivalent to 14 km of burial). The fluid composition required for this pressure estimate is XH_2O = 0.38, XCO_2 = 0.62, ± 0.07. This fluid composition is specific to one sample and may not be representative of fluid compositions in all rocks in the deposit. Metamorphic fluids were essentially a H_2O-CO_2 binary. The pressure-temperature estimate is consistent with burial metamorphism, most likely of Proterozoic age.

ACKNOWLEDGMENTS

Funding for this research was provided by Natural Sciences and Engineering Research Council of Canada grant 037233 to David R.M. Pattison. The authors wish to thank J. W. Lydon, T. Höy, and C.H.B. Leitch for their constructive reviews of this contribution. The authors also benefited from numerous discussions with other contributors to this volume.

REFERENCES

Anderson, H.E. and Parrish, R.R.
2000: U-Pb geochronological evidence for the geological history of the Belt-Purcell Supergroup, southeastern B.C.; in The Geological Environment of the Sullivan Deposit, British Columbia, (ed.) J.W. Lydon, J.F. Slack, T. Höy, and M.E. Knapp; Geological Association of Canada, Mineral Deposits Division, MDD Special Volume No. 1, p.

Bachinski, J.R.
1976: Metamorphism of cuperiferous iron deposits, Notre Dame Bay, Newfoundland; Economic Geology, v. 71, p. 443-452.

Berman, R.G.
1988: Internally-consistent thermodynamic data for stoichiometric minerals in the system Na_2O-K_2O-CaO-FeO-Fe_2O_3-TiO_2-H_2O-CO_2; Journal of Petrography, v. 75, p. 328-344.
1990: Mixing properties of Ca-Mg-Fe-Mn garnets; The American Mineralogist, v. 75, p. 328-344.
1991: Thermobarometry using multiequilibrium calculations: a new technique with petrological applications; Canadian Mineralogist, v. 29, p. 833-855.

Best, M.G.
1982: Igneous and metamorphic Petrology; W.H. Freeman and Company, New York, 690 p.

Campbell, F.A. and Ethier, V.G.
1983: Environment of deposition of the Sullivan orebody; Mineralium Deposita, v. 18, p. 39-55.

Crawford, M.L.
1966: Composition of plagioclase and assorted minerals in some schists from Vermont, USA, and south Westland, New Zealand, with inferences about the peristerite solvus; Contributions to Mineralogy and Petrology, v. 13, p. 269-294.

Connolly, J.A.D. and Cesare, B.
1993: C-O-H-S fluid compositions and oxygen fugasity in graphitic metapelites; Journal of Metamorphic Geology, v. 11, p. 379-388.

De Paoli, G.R. and Pattison, D.R.M.
1995: Constraints on temperature-pressure conditions and fluid composition during metamorphism of the Sullivan orebody, Kimberley, British Columbia, from silicate-carbonate equilibria; Canadian Journal of Earth Sciences, v. 32, p. 1937-1949.

Ethier, V.G., Campbell, F.A., Both, T.A., and Krouse, H.R.
1976: Geological setting of the Sullivan orebody and estimates of temperatures and pressure of metamorphism; Economic Geology, v. 71, p. 1570-1588.

Ferry, J.M. and Spear, F.S.
1978: Experimental calibration of the partitioning of Fe and Mg between biotite and garnet; Contributions to Mineralogy and Petrology, v. 66, p. 113-117.

Froese, E.
1969: Metamorphic rocks from the Coronation mine and surrounding area; Canadian Geological Survey, Paper 68-5, p. 55-77.

Hamilton, J.M., Bishop, D.T., Morris, H.C., and Owens, O.E.
1982: Geology of the Sullivan orebody, Kimberley, British Columbia, Canada; in Precambrian Sulphide Deposits, (ed.) R.W. Hutchinson, C.D. Spence and J.M. Franklin; Geological Association of Canada, Special Paper 25, H.S. Robinson Memorial Volume, p. 598-665.

Höy, T.
1993: Geology of the Purcell Supergroup in the Fernie West-half map-area, southeastern British Columbia; British Columbia Ministry of Energy, Mines and Petroleum Resources, Bulletin 84, 157 p.

Höy, T., Price, R.A., Legun, A., Grant, B., and Brown, D.A.
1995: Purcell Supergroup, southeastern British Columbia, compilation map; British Columbia Ministry of Energy, Mines, and Petroleum Resources, Geoscience Map 1995-1, scale 1:250 000.

Hutcheon, I.
1979: Sulphide-oxide-silicate equilibria; Snow Lake, Manitoba; American Journal of Science, v. 279, p. 643-665.

Kretschmar, U. and Scott, S.D.
1976: Phase relations involving arsenopyrite in the system Fe-As-S and their applications; Canadian Mineralogist, v. 14, p. 364-386.

Kretz, R.
1983: Symbols for rock-forming minerals; American Mineralogist, v. 68, p. 277-279.

Leech, G.B.
1957: St. Mary Lake, Kootenay District, British Columbia (82F/9); Geological Survey of Canada, Map 15-1957, scale 1:63 360.
1962: Metamorphism and Granitic intrusions of Precambrian age in southeastern British Columbia; Geological Survey of Canada, Paper 62-13, 8 p.

Leitch, C.H.B.
1992: Mineral chemistry of selected silicates, carbonates, and sulphides in the Sullivan and North Star stratiform Zn-Pb deposits, British Columbia, and in district-scale altered and unaltered sediments; in Current Research, Part E; Geological Survey of Canada Report 92-1E, p. 83-93.

Lydon, J.W. and Reardon, N.C.
2000: Sphalerite compositions of the Sullivan deposit and their implications for its metamorphic history; in The Geological Environment of the Sullivan Deposit, British Columbia, (ed.) J.W. Lydon, J.F. Slack, T. Höy, and M.E. Knapp; Geological Association of Canada, Mineral Deposits Division, MDD Special Volume No. 1, p.

Maruyama, S., Liou, L.G., and Suzuki, K.
1982: The peristerite gap in low-grade metamorphic rocks; Contributions to Mineralogy and Petrology, v. 81, p. 268-276.

McClay, K.R.
1983: Structural evolution of the Sullivan Fe-Pb-Zn-Ag orebody, Kimberley, British Columbia, Canada; Economic Geology, v. 78, p. 1398-1424.

McFarlane, C.R.M. and Pattison, D.R.M.
2000: Geology of the Mathew Creek metamorphic zone, southeast British Columbia: a window into Middle Proterozoic metamorphism in the Purcell Basin; Canadian Journal of Earth Sciences, v. 37, p. 1073-1092.

McMechan, M.E. and Price, R.A.
1982: Superimposed low-grade metamorphism in the Mount Fisher area, southeastern British Columbia - implications for the East Kootenay orogeny; Canadian Journal of Earth Sciences, v. 19, p. 476-489.

Nesbitt, B.E.
1982: Metamorphic sulphide-silicate equilibrium in the massive sulphide deposits at Ducktown, Tennessee; Economic Geology, v. 77, p. 364-378.

Read, P.B., Woodsworth, G.J., Greenwood, H.J., Ghent, E.D., and Evenchick, C.A.
1991: Metamorphic map of the Canadian Cordillera; Geological Survey of Canada, Map 1714A.

Reesor, J.E.
1973: Geology of the Lardeau map-area, east-half, British Columbia; Geological Survey of Canada, Memoir 369, 129 p.

Ross, G.M., Parrish, R.R., and Winston, D.
1992: Provenance and Pb-U geochronology of the Mesoproterozoic Belt Supergroup (northwestern United States): implications for the age of deposition and pre-Panthalassa plate reconstructions; Earth and Planetary Science Letters, v. 113, p. 57-76.

Ryan, B.D. and Blenkinsop, J.
1971: Geology and geochronology of the Hellroaring Creek Stock, British Columbia; Canadian Journal of Earth Sciences, v. 8, p. 85-95.

Schandl, E.S. and Davis, D.W.
2000: Geochronology of the Sullivan Deposit: U-Pb and Pb-Pb Ages of Zircons and Titanites; in The Geological Environment of the Sullivan Deposit, British Columbia, (ed.) J.W. Lydon, J.F. Slack, T. Höy, and M.E. Knapp; Geological Association of Canada, Mineral Deposits Division, MDD Special Volume No. 1, p.

Schandl, E.S., Davis, D.W., and Gorton, M.P.
1993: The Pb-Pb age of metamorphic titanite in the chlorite-pyrite altered footwall of the Sullivan Zn-Pb SEDEX deposit, British Columbia, and its relationship to the ore; Geological Association of Canada/Mineralogical Association of Canada, Program with Abstracts, v. 18, p. A93.

Scott, S.D.
1973: Experimental calibration of the sphalerite geobarometer; Economic Geology, v. 68, p. 466-474.

Spear, F.S.
1991: On the interpretation of peak metamorphic temperature in light of garnet diffusion during cooling; Journal of Metamorphic Geology, v. 9, p. 379-388.

Symmes, G.H. and Ferry, J.M.
1992: The effect of whole-rock MnO content on the stability of garnet in pelitic schists during metamorphism; Journal of Metamorphic Geology, v. 10, p. 221-237.

Toulmin III, P., Barton, P.B. jr., and Wiggins, L.B.
1991: Commentary on the sphalerite geobarometer; American Mineralogist, v. 78 p. 1038-1051.